Redox Biology 81 (2025) 103540

Contents lists available at ScienceDirect

Redox Biology

journal homepage: www.elsevier.com/locate/redox

Investigating neutrophil responses to stimuli: Comparative analysis of reactive species-dependent and independent mechanisms

Lorenna Rocha Reis [1], Rafaela Oliveira Nascimento [1], Mariana Pereira Massafera, Paolo Di Mascio, Graziella Eliza Ronsein [*]

Department of Biochemistry, Institute of Chemistry, University of São Paulo, São Paulo, 05508-000, Brazil

ARTICLE INFO

Keywords:
Neutrophil
NADPH oxidase activation
Degranulation
PMA
Ionomycin
Reactive oxygen species

ABSTRACT

Neutrophils play a critical role in immune response, using mechanisms as degranulation, phagocytosis, and the release of extracellular DNA together with microbicidal proteins, the so-called neutrophil extracellular traps (NETs), to combat pathogens. Multiple mechanisms might be involved in neutrophil's response to stimuli, but the biochemical characterization of each different pathway is still lacking. In this study, we used superoxide measurements, live-imaging microscopy and high-resolution proteomics to provide a thorough biochemical characterization of the neutrophil's response following activation by two well-known stimuli, namely phorbol-12-myristate-13-acetate (PMA), and ionomycin, a calcium ionophore. Our results demonstrated that although both stimuli induce extracellular DNA release, signals and mediators released by activated cells before this final event were distinct. Thus, PMA-treated neutrophils induce superoxide production, and degranulation of proteins from all granules, especially those derived from secretory vesicles and tertiary granules. On the other hand, ionomycin-treated neutrophils do not stimulate superoxide generation, but induce extensive protein citrullination (also known as arginine deimination), particularly modifying proteins related to actin cytoskeleton organization, nucleus stability, and the NADPH oxidase complex. Interestingly, many of the citrullinated proteins detected in this work were also found to act as autoantigens in autoimmune diseases such as rheumatoid arthritis. These striking differences show neutrophils' response to PMA and ionomycin are two distinct biochemical processes that point towards neutrophils diversification and plasticity responding to the environment. It also provides implications for understanding neutrophil-driven microbial response and potential roles in autoimmune diseases.

1. Introduction

Neutrophils are highly specialized cells of the innate immune system that eliminate pathogens using a range of microbicidal proteins, with or without the assistance of reactive oxygen species (ROS) [1–3]. These microbicidal proteins are primarily stored in distinct compartments called granules within neutrophil cytosol [4], and they can be released either intracellularly into the phagosome compartment or extracellularly, through degranulation or in association with DNA, in structures called neutrophil extracellular traps (NETs) [5,6].

NETs were first described to be released by neutrophils upon stimulation with phorbol-12-myristate-13-acetate (PMA), interleukin-8 (IL-8), or lipopolysaccharide (LPS), in a process culminating in a type of cell death that was later coined "NETosis" [7]. Further research showed that other stimuli also induce neutrophils to release their DNA extracellularly. Calcium ionophores, such as ionomycin, are examples of such stimuli [8,9]. Despite commonly causing DNA extrusion, different stimuli seem to induce distinct neutrophil responses, with or without the activation of superoxide production by NADPH oxidase [10–12]. The use of phorbol-12-myristate-13-acetate (PMA) and the calcium ionophore ionomycin as neutrophil's activators, may possibly represent two distinct mechanisms of neutrophil's activation [11]. PMA directly activates protein kinase C (PKC) by mimicking the action of diacylglycerol (DAG), which acts by phosphorylating the NADPH oxidase subunits, allowing for their assembly and activation [13,14]. PMA induces neutrophil degranulation [15], mild intracellular Ca^{2+} oscillations [10],

* Corresponding author. Department of Biochemistry, Institute of Chemistry, University of São Paulo, Av. Prof. Lineu Prestes, 748, São Paulo, SP, 05508-000, Brazil.
E-mail address: ronsein@iq.usp.br (G.E. Ronsein).
[1] These authors contributed equally to this work.

https://doi.org/10.1016/j.redox.2025.103540
Received 20 December 2024; Received in revised form 6 February 2025; Accepted 8 February 2025
Available online 26 February 2025

and causes chromatin swelling and decondensation [16], partially via the degrading action of neutrophil elastase (ELANE) on histones [17,18]. On the other hand, neutrophils treated with Ca^{2+} ionophores, such as ionomycin, have a substantial increase in their intracellular Ca^{2+} levels (above 1 μM) [19]. This increase elicits degranulation and hyperactivates the proteins arginine deiminase 2 and 4 (PAD2 and PAD4) [20], that catalyze the citrullination (also called deimination) of arginine residues. Citrullination modifies protein net charge, which in histones promotes chromatin decondensation [9]. However, there is still confounding evidence regarding the requirements of NADPH oxidase, and protein citrullination in neutrophil's activation by distinct stimuli [11,12,21]. Moreover, some researchers do not consider the process induced by calcium ionophores a form of NETosis, even though it culminates with DNA extrusion from cells [22]. Other authors suggest distinct stimuli commonly lead to NETs release, although possibly through different signaling mechanisms [11,12,21].

The literature is also controversial when considering the pathophysiological effects driven by NETosis. NETs are accepted as players in host defense, capturing and eliminating pathogens [23–25]. However, the uncontrolled release of NETs is also considered a source of autoantigens, and is associated to autoimmune pathologies as rheumatoid arthritis (RA) and systemic lupus erythematosus (SLE) [26–28].

In this work, we provided a deep biochemical characterization of neutrophil response to two common activators, namely PMA and ionomycin. By using measurements of superoxide release, live-imaging microscopy and mass spectrometry-based proteomics, we have shown extracellular DNA release induced by PMA and ionomycin is preceded by distinct events. Activation with PMA induced superoxide production, and mild neutrophil's degranulation, while the ionomycin-induced process is independent of reactive species, but leads to massive degranulation of primary and secondary granules, and widespread citrullination of proteins. The different mediators involved in neutrophils response to distinct stimuli raise the possibility that neutrophils may have different immune strategies depending on the received stimuli, and warrants future research regarding the roles of these cells in the immune response.

2. Materials and methods

2.1. Materials

Dextran, Hystopaque, ammonium bicarbonate, tris(hydroxymethyl) aminomethane hydrochloride (Tris-HCl), sodium deoxycholate (SDC), dimethyl sulfoxide (DMSO), ionomycin, phorbol-12-myristate-13-acetate (PMA), phenylmethanesulfonyl fluoride (PMSF), Amicon® Ultra 0.5 mL 10 kDa centrifugal filter units, Tween® 20, urea, benzonase® nuclease, and trifluoroacetic acid (TFA) were obtained from Sigma (St. Louis, MO, USA). SYTOX™ green, Hoechst 33342, and Pierce™ BCA protein assay kit were purchased from Invitrogen (Waltham, MA, USA). Dithiothreitol (DTT) and iodoacetamide (IAA) were purchased from Bio-Rad Laboratories (Hercules, CA, USA). Poly-D-Lysine, acetonitrile, and 0.1 % formic acid were obtained from Merck (Darmstadt, Germany). Trypsin was obtained from Promega (Madison, WI, USA).

2.2. Neutrophil isolation

Human neutrophils were isolated from healthy volunteers' heparinized blood using Dextran sedimentation, density centrifugation with Hystopaque 1.077 g/mL, and erythrocyte lysis with a hypotonic solution. Neutrophils were then resuspended in either PBS with 5.5 mM glucose or RPMI medium without phenol red [29]. Bright-field microscopy with May-Grünwald-Giemsa stain was used to check for the presence of eosinophils, and the sample was considered appropriate if eosinophils were <5 % of the cells. Blood collection was authorized by the Research Ethics Committee of the Faculty of Pharmaceutical Sciences at the University of São Paulo (CAAE 60860016.5.0000.0067), and informed consent was obtained from all subjects. Volunteers were screened to ensure they had no medical history of cardiovascular diseases, autoimmune disorders, diabetes, or other conditions that might affect immune cell function. They were also instructed to avoid alcohol and physical activity for 18 h before sample collection. This work has been carried out in accordance with The Code of Ethics of the World Medical Association (Declaration of Helsinki).

2.3. Measurement of extracellular superoxide

Extracellular superoxide release was measured by monitoring cytochrome *c* reduction [30]. Neutrophils (1×10^6 cells) were exposed to DMSO 0.005 % (v/v, vehicle), PMA 20 nM or ionomycin 6.7 μM with 40 μM cytochrome C and 5 mM taurine in PBS with 5.5 mM glucose [30]. Absorbances in 550 nm were obtained in 51 s intervals over a period of 30 min at 37 °C, using a microplate reader (Synergy H1, Biotek). The rate of superoxide release was calculated from the slope obtained using the linear part of the curves.

2.4. Live-imaging microscopy

Neutrophils (1.5×10^5 cells) were seeded onto a 24-well plate coated with 0.001 % poly-D-lysine and allowed to settle for 20 min at 37 °C in RPMI 1640 medium without phenol red, supplemented with 1 % antibiotic and 2 μM Hoechst 33342. Neutrophils were then treated with 0.005 % DMSO (vehicle), 20 nM PMA, or 6.7 μM ionomycin, followed by addition of 500 nM SYTOX green. During the imaging process, fluorescence signals from Hoechst 33342 and SYTOX Green were monitored in a single field of view, representing an average of 200–350 cells per well for each replicate. Images were captured every 2 min over a 120-min course at 37 °C with 5 % CO_2, using a 20x/0.4 objective on a Leica DMi8 widefield microscope and the LASX Application Software (Leica Microsystems). Each experiment was conducted in triplicate for every condition and donor, with three biological replicates collected from three independent donors.

2.5. NETs quantification

The method of quantification used in this work has been described in detail [31], and was based on previous methods [32]. Briefly, images obtained from live-imaging microscopy of neutrophils in the presence of Hoechst 33342 and SYTOX Green (respectively, a permeant and an impermeant dye to the cell membranes) were processed using ImageJ software (version 1.52p). This involved adjusting the local threshold of the 8-bit images generated by the Phansalkar or Bernsen functions and using the watershed function to separate cells. The cells were then counted and categorized based on their size in μm^2 and loss of plasma membrane integrity (SYTOX green positive cells). To determine the percentage of NETs, we calculated the ratio of cells with NETs (SYTOX green plus Hoechst 33342 positive cells) to the total number of cells (the sum of SYTOX green plus Hoechst 33342 positive cells, and Hoechst 33342-only positive cells), and then multiplied by 100. Cells had to be larger than 26 μm^2 to be counted (this procedure excludes any possible debris).

2.6. Secretome collection and cell lysis

Neutrophils (2×10^6 cells/mL) in RPMI 1640 medium without phenol red and supplemented with 1 % of antibiotic were allowed to settle for 30 min at 37 °C in 0.001 % poly-D-lysine coated 12-well plates. Next, cells were exposed to 0.005 % v/v DMSO (vehicle), 20 nM PMA, or 6.7 μM ionomycin for 30 or 90 min at 37 °C with 5 % CO_2. Then, the supernatant was collected and kept on ice. Cells were separated from the secretome through a 10-min centrifugation at 400×*g* and 4 °C. The cell pellet was washed three times with PBS followed by resuspension in

ammonium bicarbonate containing 0.1 % SDC for cell lysis. Afterwards, 100 nM PMSF was added to secretome and lysate samples. The proteins were concentrated by two cycles of centrifugation at 14,000×*g* for 15 min at 4 °C, using previously passivated 10 kDa centrifugal filter units [33]. Finally, proteins obtained from secretome and lysate samples were incubated twice with 12.5 U of benzonase for 45 min at 37 °C and 300 rpm.

2.7. Filter-aided sample preparation (FASP) for mass spectrometry

The concentration of proteins in the secretome and lysate samples was measured by the bicinchoninic acid assay (BCA). The amount of secreted proteins vary according to the stimulus, and for the secretome, the total protein quantification is shown in the supplemental methods data 1.

Then, 10 μg of secretome or lysate proteins were added to previously passivated 10 kDa centrifugal filter units [33,34], followed by three cycles of centrifugation at 14,000×*g* for 20 min with 500 μL 8 M Urea in 25 mM $(NH_4)HCO_3$. Proteins were reduced with 450 μL of 10 mM DTT in 25 mM $(NH_4)HCO_3$ for 30 min at 30 °C and 600 rpm, followed by centrifugation at 14,000×*g* for 20 min. Subsequent alkylation with 450 μL of 20 mM IAA in 25 mM $(NH_4)HCO_3$ for 45 min at 600 rpm and 25 °C in the dark was undertaken, followed by centrifugation at 14,000×*g* for 20 min. Next, residual DTT and IAA were removed by 4 cycles of 450 μL 25 mM $(NH_4)HCO_3$ addition followed by centrifugation at 14,000×*g* for 20 min (except for the last centrifugation, which took 2 min). Proteins were digested on-filter overnight at 37 °C and 100 rpm with trypsin (1:25 w/w) [34]. Peptides were eluted into a clean microtube after centrifugation at 14,000×*g* and 20 °C for 25 min, followed by two cycles of 150 μL 5 mM $(NH_4)HCO_3$ addition and centrifugation at 14,000×*g* for 20 min [34,35]. Finally, the samples were lyophilized at 25 °C, and stored at −80 °C until injection into the mass spectrometer. Before injection, each sample was resuspended in 100 μL of 0.1 % formic acid.

2.8. LC-MS/MS measurements

The peptides were analyzed using a Nano EASY-nLC 1200 coupled to an Orbitrap Fusion Lumos mass spectrometer (Thermo Fisher Scientific, Bremen, Germany). Each sample was injected into a trap column (nano Viper C18, 3 μm, 75 μm × 2 cm, Thermo Scientific) with 20 μL of solvent A (0.1 % formic acid in water) at a pressure of 500 bar. The peptides were then eluted onto a C18 analytical column (nano Viper C18, 2 μm, 75 μm × 15 cm, Thermo Scientific) at a flow rate of 300 nL/min. A linear gradient of solvent A (0.1 % formic acid in water) and solvent B (0.1 % formic acid in 80 % acetonitrile in water, v/v) was used to elute the peptides from the column. The gradient began with 5 % solvent B and increased to 28 % over 80 min, followed by an increase to 40 % B for 10 min. The column was then washed by increasing the solvent B percentage to 95 % in 2 min, and maintaining this percentage for 12 min. To prepare for the next injection, the system was re-equilibrated with 100 % solvent A.

After elution, the peptides were ionized using a nanospray Flex NG ion source (Thermo Scientific, Bremen, Germany) operating in positive electrospray mode with capillary temperature at 300 °C, and S-Lens RF level at 30 %. Ions were analyzed in a data-dependent acquisition (DDA) mode, in which the most intense ions are selected for fragmentation and detection. A MS1 scan was followed by data-dependent MS2 scans in a 3 s cycle time. Both MS1 and MS2 scans were performed in the Orbitrap analyzer. Precursor ions were fragmented by HCD with a normalized collision energy of 30, and were excluded for subsequent MS2 scans for 40 s. Monocharged ions or ions with undetermined charges were not fragmented to minimize interference. The resolution for the full scan mode was set as 120,000 (at m/z 200) and the automatic gain control (AGC) target at 5×10^5. The m/z range 350–1550 was monitored. Each full scan was followed by a data-dependent MS2 acquisition with a resolution of 30,000 (at m/z 200), a maximum fill time of 54 ms, and an isolation window of 1.2 m/z. For accurate mass measurements, the lock mass option was enabled in the MS scan using the polydimethylcyclosiloxane ion ($m/z = 445.12003$).

2.9. Study design, data analysis, and statistical testing

For live imaging microscopy experiments, after quantifying NETs, a 2-way analysis of variance (ANOVA) was conducted, followed by a Bonferroni *post hoc* test to compare each group against the control at the different time points using GraphPad Prism software.

The proteomic analyses were conducted using neutrophils from three different donors. Altogether, we used seven replicates per treatment (control (DMSO), PMA, and ionomycin), and all of them were run into MaxQuant software [36] simultaneously. The raw files of all proteomic experiments were processed using MaxQuant software [43], with proteins identified through the Andromeda algorithm [37] against the *Homo sapiens* Uniprot database (downloaded March 2022; 20,401 entries). The precursor and fragment error mass tolerances were set at 4.5 ppm and 20 ppm, respectively, with cysteine carbamidomethylation as fixed modification. The variable modifications included methionine oxidation, N-terminal acetylation, and deamination of arginine residues (citrullination, set as an increase of +0.98401 Da with a neutral loss of 43.0058 Da (HCNO) in arginine residues [38]). Because neutrophils release many proteases, the identification process was conducted with a semi-tryptic digestion mode, allowing a maximum of 2 missed cleavages, and a maximum FDR of 1 % for both peptides and proteins identification. Semi-specific search provides a higher number of identified proteins when compared with specific digestion, but this did not impact the downstream analyses, as the overall results remained consistent. For proteins, the false discovery rate (FDR) was calculated using a decoy database. For a protein to be considered present in a sample, at least two peptides (one of which must be unique) needed to be detected. The match between runs option was enabled, and all other parameters were maintained at their default settings. Protein abundance was calculated using the LFQ algorithm [39] present in MaxQuant software.

We used Perseus software (version 1.6.15.0) to analyze the protein data [40], and the resulting figures were generated using either GraphPad Prism (version 9.05), Perseus, or R (version 4.2.0). Volcano plots were made with the web app VolcaNoseR (https://huygens.science.uva.nl/VolcaNoseR/) [41]. Before statistical analysis, label-free quantification (LFQ) intensities were processed in Perseus software [40]. The proteins identified only by modified sites, matching the reverse and potential contaminants databases were removed via filtering. The remaining data were log2-transformed. Missing values were filtered using the criteria of at least 6 valid values in each group. A protein was considered unique (exclusive) to a group if it had at least 3 out of 7 valid values in that group and 0 or 1 valid values in the other groups. For PCA analysis, the remaining missing values after filtration were imputed with values from the normal distribution (width: 0.3 and downshift 1.8). PCA calculations and graphics were performed on R (version 4.2.0). To compare statistically significant proteins secreted under neutrophil's distinct treatments, log2-transformed LFQ protein intensities were analyzed using ANOVA with p-values adjusted based on a permutation-based false discovery rate (FDR) of 0.05. Significantly altered proteins were subsequently z-score normalized and clustered to identify patterns. Perseus software was used for hierarchical clustering of significantly altered proteins, and this clusterization was performed without imputation, and displayed as a heatmap. The Euclidean distance was used, and the average linkage method was employed to construct the rows and columns trees. For pairwise comparisons, log2-transformed LFQ protein intensities from the two treatment groups were analyzed using an unpaired *t*-test. The results were adjusted for multiple comparisons using permutation-based FDR <0.05, and the data are presented in volcano plots as log2 fold-change plotted against the -log10 of the p-value.

For analysis of citrullinated proteins, the peptides with a

citrullinated arginine in the C-terminal were considered a false-positive and manually excluded from data [31,38]. Citrullination sites at peptides from potential contaminants were also excluded from the analysis. In addition, peptides with citrullinated arginine only in one of three individuals were also removed. Common citrullinated proteins from secretome or lysate samples had to have at least 3 valid values in each treatment group (total samples from control, ionomycin, and PMA). Exclusive citrullinated proteins had to have at least 3 valid values in a treatment group and 0 or 1 in the other groups.

To investigate the subcellular locations, protein localization information was retrieved from UniProt annotations and the cellular components of Gene Ontology. According to the databases, the proteins were classified in: Cytoplasm, cytoskeleton, cytoplasmatic granule, membrane, endoplasmatic reticulum, mitochondria, nucleus, secreted or Golgi apparatus. To investigate enriched pathways we employed the g:Profiler web platform [42]. We set gene ontology biological processes and cellular components as data sources and selected the highlight driver terms in gene ontology. The significance threshold g:SCS was set as 0.05. Protein symbols were derived from gene symbols as per the recommendations of the Human Genome Organization Gene Nomenclature Committee [43], and were written in all capital letters and not italicized.

2.10. Data availability

The mass spectrometry proteomics data have been deposited to the ProteomeXchange Consortium via the PRIDE [44] partner repository with the dataset identifier PXD057968.

3. Results

3.1. Only PMA activates NADPH oxidase although both stimuli are able to induce extracellular DNA release

Control neutrophils, or those challenged with 6.7 μM ionomycin or 20 nM PMA were first compared regarding their ability to generate extracellular superoxide. The production of extracellular superoxide was assessed using the cytochrome *c* reduction assay. Neutrophils treated with ionomycin or unstimulated (control) do not generate appreciable amounts of superoxide (Fig. 1A). In contrast, neutrophils treated with PMA released superoxide at a rate of 4.9 ± 1.3 μM/min. Consistent with previous reports [12,45], our findings show that PMA is a strong activator of NADPH oxidase. In the conditions of our experiment, ionomycin treatment did not induce NADPH oxidase activation.

Given the striking differences regarding NADPH oxidase activation (measured as superoxide production) upon different stimuli, we next sought to study the ability of each stimulus to induce NETs release. With that in mind, neutrophils treated with 0.005 % (v/v) DMSO (Control), 6.7 μM ionomycin, or 20 nM PMA in the presence of Hoechst 33342 and SYTOX Green were monitored with live-imaging microscopy for 120 min (Fig. 1B). This experimental design allowed us to observe the release of NETs, as indicated by the uptake of the impermeant SYTOX Green dye, while also visualizing the morphology of the cells using the permeant Hoechst 33342 dye. Thus, our results demonstrate that both PMA and ionomycin are capable of inducing NETosis, albeit with different kinetics (Fig. 1B and C). Notably, approximately 30 % of the neutrophils treated with ionomycin already underwent NETosis at 60 min (Fig. 1B and C), and at the time point of 90 min (Fig. 1B), all ionomycin-treated

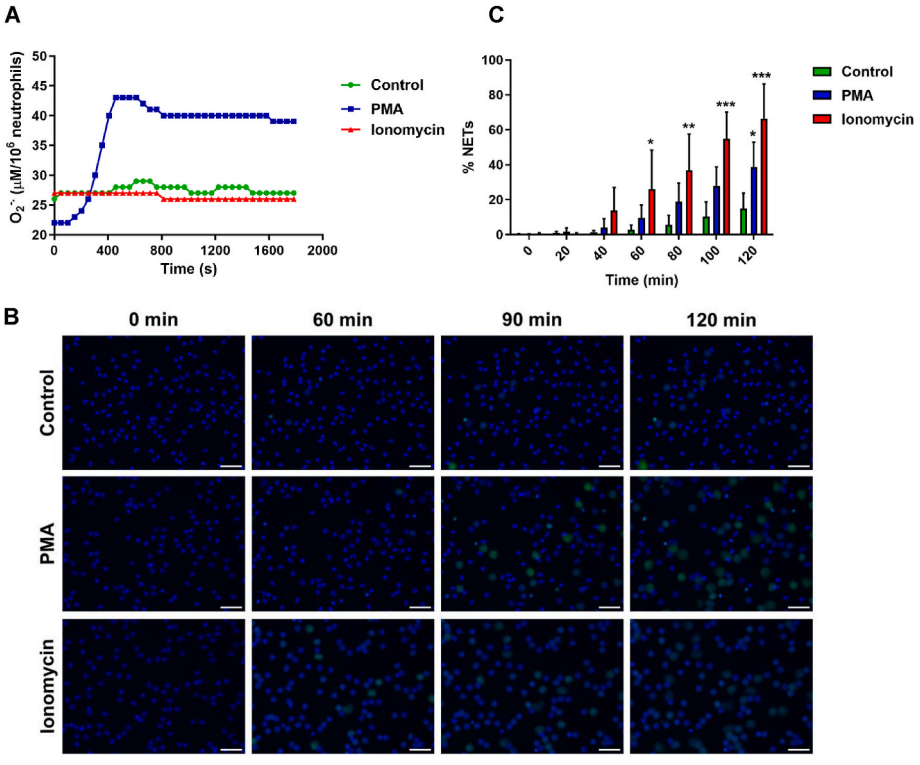

Fig. 1. The generation of superoxide and NETs release kinetics are stimulus-dependent. Neutrophils were treated with 0.005 % (v/v) DMSO (control), 20 nM PMA or 6.7 μM ionomycin. (A) The superoxide production was measured through the reduction of 40 μM cytochrome C at 37 °C in the presence of 5 mM taurine. Superoxide concentration was calculated by dividing the absorbance at 550 nm by the molar absorptivity of 21,000 M^{-1} cm^{-1}, and considering the path length of 1 cm. Absorbance measurements were taken at intervals of 51 s. To analyze the formation of NETs, the neutrophils were stained with 2 μM Hoechst 33342 (blue, cell permeant dye) and 500 nM Sytox Green (green, cell impermeant dye), and monitored for 120 min at 37 °C and 5 % CO_2 in the microscope. Images are representative of three independent experiments with neutrophils isolated from different volunteers. (B) Microscope images of untreated and treated neutrophils at different time points. Scale bars represent 50 μm. (C) The percentage of neutrophils that released NETs, defined as Hoechst 33342 and SYTOX Green (+) cells was calculated over time with respect to all neutrophils (all cells >26 μm^2 that were either Hoechst 33342 (+) only, or Hoechst 33342 (+) and SYTOX Green (+)).

cells exhibited either a decondensed nucleus (loss of the polymorphic shape) or the presence of NETs. In contrast, after 90 min of treatment with PMA, only a few neutrophils exhibited NETs, while some still displayed the characteristic polymorphic nucleus (Fig. 1B and C). At the time point of 120-min, approximately 40 % of PMA-treated neutrophils displayed NETs, contrasting with approximately 65 % of ionomycin-treated neutrophils (Fig. 1C). These findings demonstrate that PMA and ionomycin are potent inducers of extracellular DNA release, with ionomycin-treated neutrophils inducing a faster release of NETs.

3.2. The neutrophil's response after activation is stimulus-dependent

The results obtained so far pointed to a dissimilar response of neutrophils to distinct stimuli. We then used a proteomic approach to investigate the proteins secreted by controls, or by neutrophils treated with 6.7 μM ionomycin, or 20 nM PMA for 30 and 90 min. The total protein quantification is shown in the supplemental methods data 1.

Initially, a dimensionality reduction analysis revealed three main clusters in our dataset (Fig. 2A). The first cluster was composed of the neutrophils stimulated for 30 and 90 min with PMA, the second cluster was composed of controls for both time points, and the third contained samples obtained after treatment with ionomycin for 30 and 90 min (Fig. 2A). The first two components explained approximately 55 % of the variance of the whole dataset. This first exploratory analysis already revealed that secretion of intracellular proteins is stimulus-dependent and do not vary considerably in composition with time, since for each different stimulus, 30 and 90 min-time points are in relatively close proximity in the principal component analysis (Fig. 2A).

The unsupervised hierarchical clustering of the significantly altered proteins ($P < 0.05$ after ANOVA adjusted for multiple comparisons, FDR<0.05) confirmed the separation of samples into three major treatment clusters (Fig. 2B, columns). The first cluster represents the secretome of neutrophils treated with PMA (for either 30 or 90 min, blue boxes), the second cluster comprises the ionomycin-stimulated neutrophil's secretome (red boxes), and the last cluster displays samples from the control group (green boxes) (Fig. 2B). Importantly, these results show that response to different stimuli is common for all 3 volunteers, since samples clustered by treatment (control, PMA, or ionomycin), but not by donor. Also, clusterization by treatment and not by time reinforces that for each stimulus, a similar set of proteins are secreted over time. The protein abundances across treatments (rows) were partitioned into four major clusters: proteins enriched in the control and ionomycin groups (cluster 1), those enriched mainly in the ionomycin group (cluster 2), those enriched in the control group (cluster 3), and those enriched in the PMA group (cluster 4) (Fig. 2B and Supplemental Table 1A). We also categorized the number of unique and shared proteins among treatments using a Venn diagram (Fig. 2C), which revealed that the majority of the secreted proteins (n = 320) are shared among them.

Aiming to understand the secretion pattern present upon activation of neutrophils with distinct stimuli, subcellular location analysis was conducted by combining the proteins obtained from each cluster in

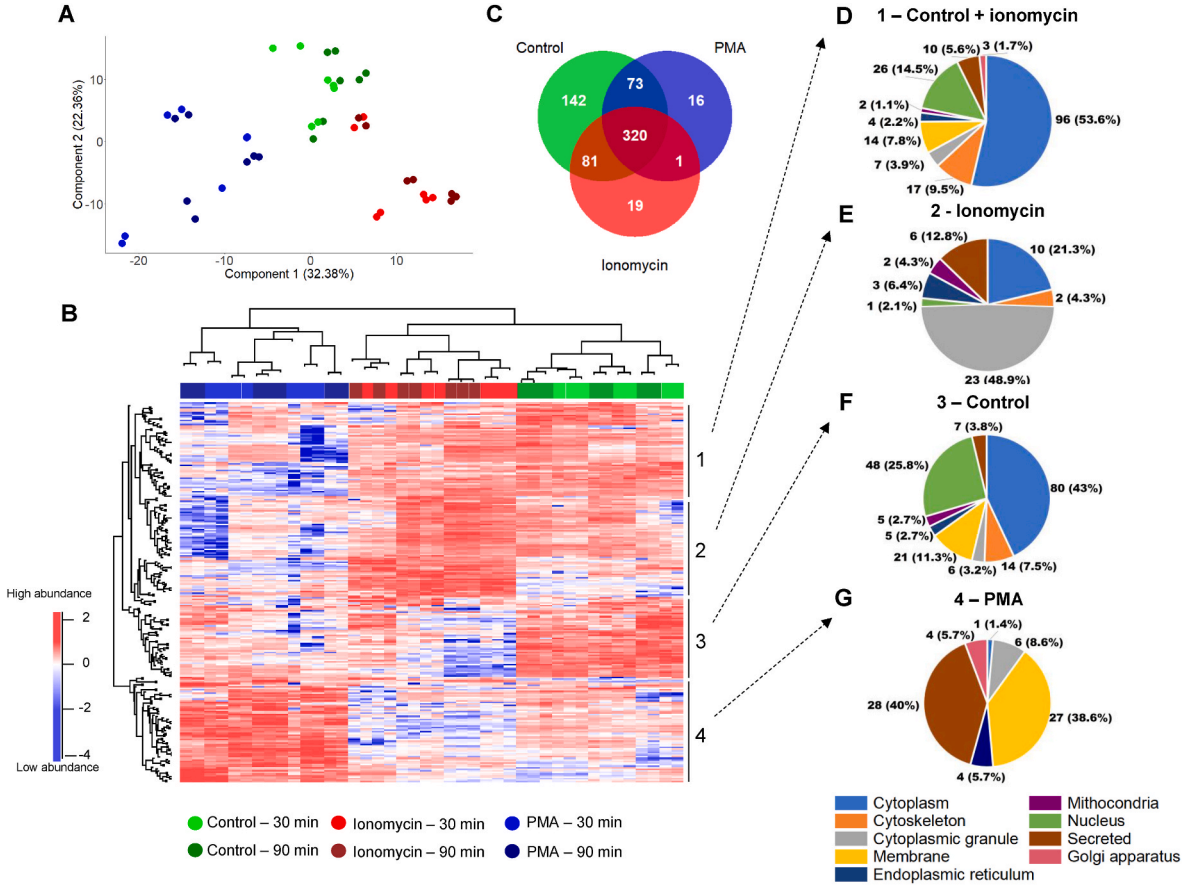

Fig. 2. Neutrophils treated with PMA or ionomycin secreted proteins involved in cell homeostasis and immune response. The secretome of neutrophils treated with 0.005 % v/v DMSO (Control), 20 nM PMA, or 6.7 μM ionomycin for 30 and 90 min at 37 °C was collected, processed and analyzed by mass spectrometry. A) Principal component analysis (PCA) of the secretome of neutrophils exposed to different stimuli for 30 or 90 min. B) Hierarchical clustering of significantly altered proteins (ANOVA corrected for multiple comparisons using FDR<0.05). C) Venn diagram of proteins identified in each group. Subcellular location analysis of the unique and enriched proteins found in D) control and ionomycin groups, E) ionomycin group, F) control group, and G) PMA group. Secretome proteins were obtained from neutrophils in three independent experiments.

Fig. 2B (and Supplemental Table 1A) with the unique proteins of the same group identified in the Venn diagram in Fig. 2C (and Supplemental Table 1A).

For example, in the heatmap (Fig. 2B), proteins from cluster 1 (proteins enriched in ionomycin and control treatments) were combined with proteins exclusively found in control and ionomycin samples from the Venn diagram (n = 81, Fig. 2C), and subcellular location (Fig. 2D and Supplemental Table 1B) and cellular component (Supplemental Table 1B) analyses were performed. The results show that ionomycin-stimulated neutrophils and controls commonly secrete proteins linked to actin filament organization, cell motility, and adhesion (Supplemental Table 1B). This is expected, since isolated neutrophils, despite being circulating cells in the organism, adhere to the cell culture plates during the experiment. Subgroup analysis comparing the secretome of control and ionomycin-treated neutrophils showed the majority of proteins secreted by control neutrophils (75 %) are actually for secretion, or belong to the cytoplasm (including extracellular exosomes and proteins present in extracellular regions), membrane, and cytoskeleton (Supplemental Fig. 1 and Supplemental Table 1C). On the other hand, the majority of proteins enriched in the secretome of ionomycin-treated cells (36.5 %) originated from cytoplasmic granules. Examples of such proteins are MPO, bactericidal permeability-increasing protein (BPI), proteinase 3 (PRTN3), and lysozyme C (LYZ) (Supplemental Fig. 1 and Supplemental Table 1C). These results agree with a recent study that showed neutrophils secreted proteins from primary and secondary granules as early as 2 min after ionomycin treatment [31].

The joint analysis of proteins from cluster 2 in the heatmap (Fig. 2B and Supplemental Table 1A), and proteins secreted only by ionomycin-activated neutrophils from the Venn diagram (n = 19, Fig. 2C and Supplemental Table 1A), shows that the secretome of ionomycin-activated neutrophils follows the same pattern obtained in the subgroup analysis comparing ionomycin-treated and control samples. Thus, secretome of ionomycin-activated neutrophils is enriched in proteins originating from cytoplasmic granules (48.9 %), including many proteins belonging to the azurophil granule as beta-hexosaminidase subunit alpha (HEXA), beta-hexosaminidase subunit beta (HEXB) and LYZ (Fig. 2E and Supplemental Table 1D).

Data from cluster 3 in the heatmap (Fig. 2B–Supplemental Table 1A), representing proteins secreted in higher abundance on the control group, were combined with proteins exclusively secreted by the control cells from the Venn diagram (n = 142, Fig. 2C–Supplemental Table 1A). The proteins in this cluster (Fig. 2F and Supplemental Table 1E) are from actin cytoskeleton, adherent junctions, collagen-containing extracellular matrix, such as alpha cardiac muscle actin 1 (ACTC1), actin alpha 1 (ACTA1), actin alpha 2 (ACTA2), actin beta (ACTB), vimentin (VIM), cofilin-1 (CFL1, an actin binder), and annexins (i.e. ANXA5, ANXA6) as previously reported [31]. Secretion of proteins associated to cytoskeleton and adherence by control neutrophils likely reflects their adhesion to poli-D-lysine plates before treatment. In stimulated cells, these proteins may be less detectable due to the proteins secreted in response to the activation processes.

The enrichment analysis obtained by combining proteins of cluster 4 in the heatmap (Fig. 2B and Supplemental Table 1A) with proteins secreted by PMA-treated neutrophils from the Venn diagram (n = 16, Fig. 2C and Supplemental Table 1A) showed the majority of proteins in PMA-treated neutrophil's secretome are designated for secretion (40 %) or belong to membrane or cell surface (38.6 %) (Fig. 2G). Importantly, many proteins annotated by the GO as membrane proteins are also from neutrophil granules (they are highlighted in yellow in Supplemental Table 1F). A closer look reveals such proteins are primarily involved in the immune response. Examples of these proteins include integrin beta-2 (ITGB2) that has been related to positive regulation of superoxide production, and only observed in the PMA-activated neutrophils [46] and the proteases MMP8 and MMP9 (Fig. 2G and Supplemental Table 1F).

3.3. PMA- and ionomycin-activated neutrophils exhibit distinct patterns of degranulation

Our global analysis of the secretome of stimulated neutrophils showed that they release proteins according to the stimulus. Intriguingly, our results also showed ionomycin-stimulated cells release NETs much faster than PMA-activated neutrophils (Fig. 1B and C). A key question that remained to be answered is if PMA-activated neutrophils are slower in the process of NETosis, but still release the same signals as ionomycin-treated neutrophils, or if the entire process unraveled by activation is different. To gain insights into this matter, we performed a subgroup analysis comparing the secretome of ionomycin-activated neutrophils after 30 min with that obtained after 90 min of PMA activation, i.e., time-points before NETs release by these stimuli. We chose this subgroup comparison for two reasons. First, the lobular nuclear shape of PMA-treated neutrophils has not changed even after 60 min of incubation, and after 90 min, NETosis has occurred only in approximately 20 % of cells, while approximately 40 % of ionomycin-treated neutrophils already underwent NETosis at this time point. This is important to avoid confounding factors such as significant cell death and the associated release of intracellular contents. Second, we performed a cellular component comparison between proteins secreted by ionomycin-stimulated neutrophils after 30 and 90 min of incubation (Supplemental Fig. 2A). The results show an increase in intracellular proteins with increasing incubation time, suggesting that a higher number of cells have lost membrane integrity releasing intracellular components. This result corroborates the one obtained in Fig. 1. On the other hand, the composition of secreted proteins after 30 or 90 min of PMA activation does not change considerably, reinforcing the results obtained with microscopy that show majority of cells remains intact after 90 min (Supplemental Fig. 2B).

Thus, 692 secreted proteins were identified comparing the secretome of ionomycin-activated neutrophils after 30 min with that obtained after 90 min of PMA activation (Fig. 3A and Supplemental Table 2A). From this total, 445 proteins (64.3 %) were common between the groups, 141 proteins (20.4 %) were exclusive to the ionomycin group, and 106 proteins (15.3 %) were exclusive to the PMA group. We then tested whether or not the abundance of the common proteins secreted after 30 min of ionomycin treatment was the same when comparing with proteins secreted after 90 min of PMA stimulus (Fig. 3B and Supplemental Table 2B). All proteins with a fold-change greater than 2 ($Log_2 > 1$) and significantly altered ($P < 0.05$) after a multiple comparison adjusted *t*-test, were color-coded either red (ionomycin group) or blue (PMA group). The ionomycin-treated neutrophils exhibited a 4-fold enrichment in BPI, and a 2.5-fold enrichment in MPO, proteins present in the neutrophil's azurophilic granule (Fig. 3B and Supplemental Table 2B). In addition, the neutrophils treated with ionomycin showed enrichment of azurophilic proteins HEXA, HEXB, and Mannosidase Alpha Class 2B Member 1 (MAN2B1) [47,48]. They also show a 3.2-fold increase in the calprotectin subunit protein S100-A8 (S100A8) and a 2.7-fold increase in protein S100-A9 (S100A9), which extracellularly also have antimicrobial activity (Fig. 3B and Supplemental Table 2B).

Conversely, following a 90-min treatment with PMA, the neutrophils' secretome exhibited significant enrichment in proteins from tertiary and ficolin granules, beside secretory vesicle components, such as ITGAM (3.3-fold increase), ITGB2 (3.6-fold increase), glutaminyl-peptide cyclotransferase (QPCT, 3.2-fold increase), ficolin-1 (FCN1, 3.3-fold increase), and CD177 antigen (CD177, 1.3-fold increase) (Fig. 3B and Supplemental Table 2B). Notably, ITGAM, ITGB2, and CD177 also positively regulate superoxide generation by NADPH oxidase [46,49]. The PMA-treated cells' secretome also showed an increase in MMP8 (1.3-fold increase) and MMP9 (1.5-fold increase), extracellular matrix proteases that degrade collagenase and gelatinase [50], facilitating neutrophil extravasation (Fig. 3B and Supplemental Table 2B).

To gain a better understanding of the cellular process and molecular function of the proteins being secreted by each stimulus, we combined

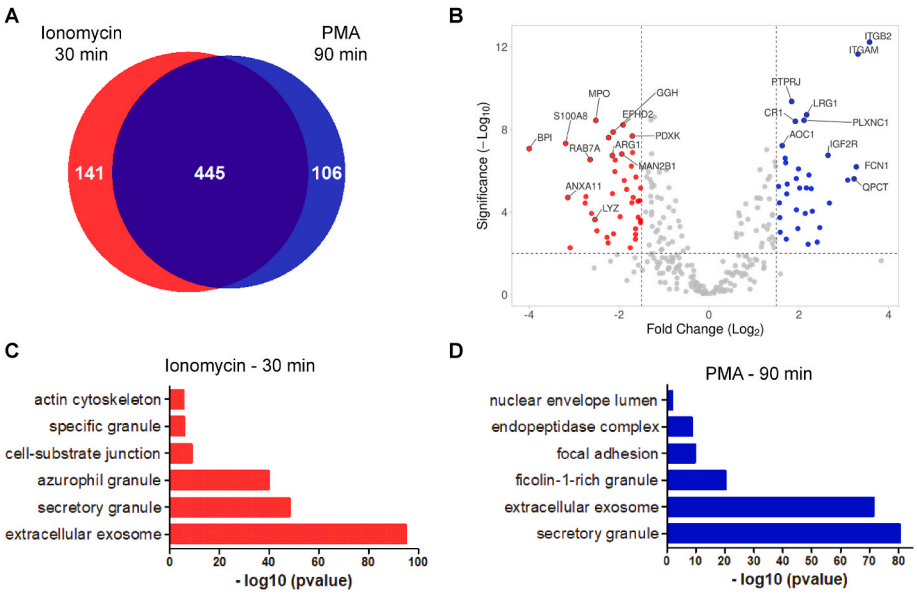

Fig. 3. Different patterns of degranulation are seen in ionomycin- and PMA-treated neutrophils. The secretome of human neutrophils treated with 6.7 μM ionomycin for 30 min or 20 nM PMA for 90 min at 37 °C was analyzed by mass spectrometry. A) Venn diagram of proteins commonly or exclusively identified in the secretome of neutrophils treated with ionomycin for 30 min or PMA for 90 min. B) Differentially regulated proteins obtained comparing ionomycin- and PMA-treated neutrophils at 30 and 90 min, respectively. The log2 fold change between the ionomycin and PMA treatment groups is plotted against the -log10 of the P value obtained from the *t*-test, which was followed by multiple comparisons adjustment. Proteins more abundant in the secretome of ionomycin-treated neutrophils are displayed to the left of the value −1 in the x-axis (dashed line), while proteins more abundant in the PMA group are displayed to the right of the 1 value. Cellular component analysis of the unique and enriched proteins found in the secretome of C) ionomycin or D) PMA stimulated neutrophils. Only cellular components with FDR <0.05 were displayed. Annotations were derived from GO terms, which may include broad or nonspecific classifications in the context of neutrophil biology. Secretome proteins were obtained from neutrophils in three independent experiments.

the enriched (Fig. 3B and Supplemental Table 2B) and unique proteins (Fig. 3A and Supplemental Table 2A) of each group and performed a cellular component analysis (Fig. 3C and D, and Supplemental Tables 2C and 2D). The results show the secretome of neutrophils after 30 min exposure to ionomycin is enriched with proteins from the azurophil granule, and from the specific and secretory granules. On the other hand, after 90 min, the secretome of PMA-treated neutrophils is enriched with proteins from the extracellular exosome, secretory, and ficolin-1-rich granules. Of note, proteins such as catalase, superoxide dismutase, S100 subunits, and peroxiredoxins, generally considered to be cytoplasmic or localized to other compartments in resting cells, were cataloged in exosomal fractions in situations involving cellular stress, activation, or oxidative signaling. This underscores a key limitation of functional annotations based on global databases such as gene ontology, which may include broad or nonspecific classifications that do not that accurately reflect neutrophil biology. Specific and tertiary granules share many protein with secretory vesicles, but have different pathogen-recognition receptors and additional adhesion molecules [47,51,52]. Furthermore, they contain proteins that make the surrounding tissue inhospitable for pathogens, such as gelatinase and collagenase, and a few microbicidal proteins [47].

In summary, both treatment groups secrete proteins derived from the extracellular exosome and proteins from the secretory vesicles. However, ionomycin-treated neutrophils released more proteins from the azurophil and specific granules, and proteins associated with actin cytoskeleton. Of note, proteins enriched in PMA-activated neutrophils are related to neutrophil extravasation and superoxide production. The observed differences in degranulation between the treatment groups are additional evidence that the processes triggered by PMA or ionomycin are distinct.

3.4. Ionomycin induces extensive citrullination of cellular proteins

Neutrophil activation by ionomycin leads to an increase in the levels of Ca^{2+} in the cells [29], associated with the activation of the PAD4 enzyme, capable of converting arginine residues into citrulline (citrullination) [20]. The presence of citrullinated proteins is a characteristic of PAD4 activation, and protein hypercitrullination was associated with NETs formation independent of NADPH oxidase activation [9]. Thus, we analyzed the secretome and the lysate of the neutrophils to investigate the presence of protein citrullination within different treatment groups.

We detected 28 citrullinated proteins in the secretome of neutrophils, most of them from the cells treated with ionomycin. Twelve proteins were exclusively citrullinated in this group, representing almost 43 % of the secreted citrullinated proteins (Fig. 4A, Supplemental Table 3A). Neutrophils treated with PMA or control shared 4 citrullinated proteins and the control group had 2 exclusively citrullinated proteins (Fig. 4A–Supplemental Table 3A). The higher number of citrullinated proteins in the secretome of neutrophils activated by ionomycin can be related to higher activation of the PAD4 enzyme [19].

We also analyzed the presence of citrullinated proteins in the lysate of the neutrophils. Similar to the secretome, the neutrophils activated by ionomycin showed enhanced citrullination. In total, we observed 135 proteins citrullinated in the lysate of neutrophils (Fig. 4B and Supplemental Table 3B). The majority of the proteins were exclusive to the ionomycin group with 126 proteins, only one protein was exclusively citrullinated in the PMA group while another was shared with the control group. Of interest, levels of PAD4 (measured by proteomics) were unaltered across treatments (data not shown).

To track cellular components (Fig. 4C and Supplemental Table 3C) and biological processes (Fig. 4D and Supplemental Table 3D) of citrullinated proteins in ionomycin-treated neutrophils, we performed a pathway enrichment analysis combining citrullinated proteins from the ionomycin group in the secretome and lysate samples. In agreement with what was previously described [31,38], we observed citrullination of proteins related to cytoskeleton organization (Fig. 4C and D), such as vasodilator-stimulated phosphoprotein (VASP), coronin-1A (CORO1A),

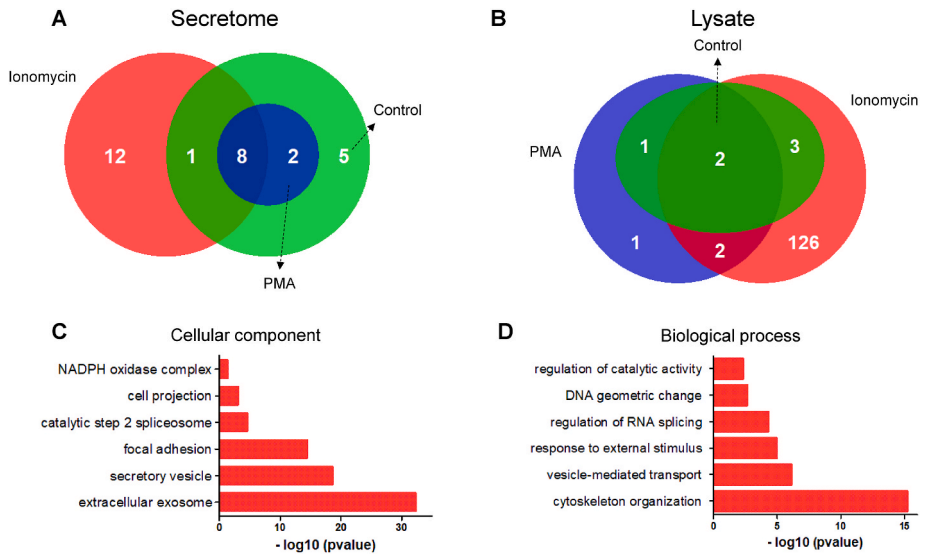

Fig. 4. Protein citrullination in the secretome and lysate of neutrophils activated by different stimuli. Neutrophils were treated with 6.7 μM ionomycin for 30 min and 0.005 % v/v DMSO or 20 nM PMA for 90 min at 37 °C. The secretome and lysate were collected, processed and analyzed by mass spectrometry. Venn diagram of citrullinated proteins detected in the (A) secretome or (B) lysate in the cells treated with different stimuli. Cellular components (C) and biological process (D) for citrullinated proteins found in the secretome and lysate of neutrophils activated by ionomycin. Annotations were derived from GO terms, which may include broad or nonspecific classifications in the context of neutrophil biology.

VIM, delta (14)-sterol reductase (LBR) and lamin B1 (LMNB) (Supplemental Tables 3C and 3D) [31,53]. The last three proteins are also related to the structure and stability of the neutrophil nucleus [54–57] and were suggested as part of the NETs formation in neutrophils activated by ionomycin (Supplemental Table 3B) [31,53].

Interestingly, three of the citrullinated proteins enriched in the process related to response to external stimulus, and the cellular component "NADPH oxidase complex" were the proteins neutrophil cytosolic factor 1 (NCF1), neutrophil cytosolic factor 2 (NCF2), and cytochrome *b*-245 light chain (CYBA) (Fig. 4C and D, Supplemental Tables 3C and 3D). The proteins NCF1 and NCF2 are the cytosolic components of the enzyme NADPH oxidase, and CYBA is one of the membrane components of the enzyme [58]. Of note, a previous report showed that citrullination of components of NADPH oxidase complex prevented both its activation and superoxide production [59].

Protein citrullination has been associated with several autoimmune diseases as rheumatoid arthritis (RA) and multiple sclerosis [60]. In RA, the citrullinated proteins can act as autoantigens and anticitrullinated protein antibodies (ACPA) specifically target these modified proteins [61]. Notably, citrullinated forms of proteins like α-enolase, VIM, and fibrin have been identified as key targets for ACPAs, but many other citrullinated proteins have been identified in synovial fluid and tissue of RA patients [62]. In our study, we detected numerous citrullinated proteins, several of which have been previously identified in samples of patients with RA. We observed the same citrullination sites in VIM and also in ACTB, ALDOA, CORO1A, heat Shock Protein 90 Alpha Family Class A Member 1 (HSP90AA1), myosin 9 (MYH9), MNDA, and TLN1 [61,63,64].

In summary, the neutrophils treated with ionomycin had more citrullinated proteins in their secretome and lysate. As previously observed, the proteins citrullinated in the ionomycin-treated cells were related to cytoskeleton organization and nucleus stability. Also, some of the citrulinated proteins in the ionomycin group are part of the NADPH complex. The modification of these proteins could be involved in the lack of superoxide production by neutrophils treated with ionomycin. Interestingly, we detected citrullinated proteins that were previously identified in samples of RA individuals and could act as antigens in the disease.

4. Discussion

For a long time, PMA and calcium ionophores have been used *in vitro* as surrogate stimuli to mimic neutrophil activation in the circulation. Both stimuli are reported to induce neutrophils' DNA release [65–67]. However, there are conflicting results in the literature regarding the biochemical mechanisms that occur under each distinct neutrophil stimulus. While some authors postulate that DNA release can occur through concomitant activation of NADPH oxidase, histone citrullination, and membrane rupture [68], others believe that the processes induced by PMA and calcium ionophores are completely distinct and the later stimulus do not induce NETs release [22]. Instead, these authors propose that ionophores induce a process called leukotoxic hypercitrullination that is unrelated to NETs [22,62].

In this work, we provided direct evidence that PMA and ionomycin activation of neutrophils proceed through distinct biochemical pathways. Our studies using live imaging microscopy, superoxide measurements and mass spectrometry-based proteomics showed both stimuli eventually lead to membrane rupture and DNA released extracellularly, but the process is much faster under ionomycin activation. Mechanistically, only PMA-treated neutrophils activate the NADPH oxidase. On the other hand, only ionomycin was able to induce widespread protein citrullination. Finally, although both stimuli lead to degranulation, ionomycin caused a massive release of proteins from primary and secondary granules, unparalleled by PMA effects.

Consistent with earlier reports, treatment of neutrophils with PMA resulted in the generation of superoxide by NADPH oxidase, and the release of NETs after 120 min [10–12]. A similar response was described in neutrophils treated with pathogens, including *P. aeruginosa*, *S. aureus*, and *E. coli* [12,69]. PMA-induced NETs are diminished using neutrophils from individuals with chronic granulomatous disease (CGD), who cannot produce superoxide by NADPH oxidase, and from neutrophils treated with the flavoprotein inhibitor diphenyleneiodonium (DPI) [12,69]. Reactive oxygen species are believed to be essential for NETs formation, participating in MPO-dependent translocation of neutrophil elastase from granules to the nucleus, and subsequently leading to histone acetylation and NETs release [18].

In contrast, neutrophils treated with ionomycin were not able to activate the NADPH oxidase, but they still released DNA extracellularly.

The independence of NADPH oxidase activation for NETosis has already been described for calcium ionophores such as ionomycin and A23187 [10,11,70], and a similar response was observed in neutrophils treated with *C. albicans* [71], soluble immune complexes [72], *S. aureus*, or monosodium urate crystals [32]. Much of the response observed in the ionomycin-treated neutrophils can be related to the increase in the calcium intracellular concentration. One enzyme activated in these conditions is PAD4, which can citrullinate arginine residues [73]. Importantly, the majority of studies involving NETs caused by ionophores relate NETosis to the citrullination of a single protein, the histone H3 [9,11,74]. We and others have previously shown citrullination is a widespread cellular event, and proteins related to actin cytoskeleton and nucleus stability were found citrullinated upon ionomycin treatment [31,38]. These results were further confirmed in this work. Significantly, we have showed citrullination occurs almost exclusively in ionomycin-treated neutrophils, with controls and PMA-activated cells exhibiting low citrullination levels. Importantly, upon neutrophils activation, the cytosolic components of NADPH oxidase migrate to the membrane where they form a complex with the membrane components resulting in the active form of the enzyme [14,58]. Recently, it was shown that in resting neutrophils the enzymes PAD4 and the cytosolic components of NADPH oxidase are associated. The citrullination of NCF1 and NCF2 causes their dissociation from PAD4 and the NADPH oxidase complex is not formed [59]. Our results corroborate these observations, and may provide a likely mechanism for the lack of NADPH oxidase activation, since neutrophils stimulated by ionomycin displayed citrullination of NCF1 and NCF2 components of NADPH oxidase (Supplemental Tables 3A and 3B), and these cells did not generate measurable amounts of superoxide ion (Fig. 1A). However, these observations need to be confirmed in future studies. In striking contrast, PMA-treated cells have a sustained generation of superoxide (Fig. 1A), and no citrullination of NCF1 or NCF2 was detected.

Besides protein hypercitrullination, we also showed neutrophils activated by ionomycin release extracellularly proteins belonging to all their granules, likely due to the rise in the intracellular calcium levels. The uncontrolled release of several granule proteins seen upon ionomycin treatment can act as autoantigens in systemic autoimmune diseases. The secretion of MPO, PRTN3, and cathelicidin (CAMP), either alone or in association with NETs, can serve as antigens in anti-neutrophil cytoplasmic antibody-associated vasculitis, and systemic lupus erythematosus (SLE) [27,28,75]. Moreover, citrullinated proteins have been shown to act as autoantigens in diseases like RA, where anticitrullinated protein antibodies (ACPA) have been consistently detected [76]. Interestingly, many of the citrullinated proteins identified in this work were also observed in the synovial fluid of RA patients, indicating that activation of neutrophils by this pathway might be a common mechanism implicated in autoimmune disease progression. Neutrophils exposed to pore-forming toxins from different bacteria express the same increase in calcium levels intracellularly, followed by protein citrullination and DNA release [77,78]. Moreover, host perforin, a protein secreted by natural killer cells and cytotoxic lymphocytes [79,80], also forms pores in the cell membrane, allowing free influx and efflux of ions (including calcium). Thus, it has been suggested that the damage caused by pore-forming microbials may stimulate chronic hypercitrullination in neutrophils, leading to ACPA production, and leading to RA development in susceptible individuals [62].

While our study provides valuable insights into neutrophil responses upon distinct stimuli, it also has some limitations. First, neutrophils are highly sensitive to *ex vivo* manipulation, and it is a challenge to establish a true control baseline that accurately reflects their *in vivo* unstimulated state. Despite our efforts to standardize experimental conditions, including the use of freshly isolated neutrophils, unstimulated neutrophils may not serve as the ideal control for all aspects of the study. In addition, a significant challenge when studying neutrophils is their inherent heterogeneity [81]. There are various forms of neutrophil heterogeneity. Of special interest is the low-density granulocyte (LDG) population found in patients with SLE [82–84]. These neutrophils have an activated phenotype secreting inflammatory cytokines and releasing more NETs, but show impaired phagocytic potential. While our study did not directly examine heterogeneity within neutrophil population, the functional differences we observed in response to PMA and ionomycin treatments may reflect the contributions of distinct subpopulations within the broader neutrophil pool. It is important to note that our proteomics data represent the average protein abundance across the entire neutrophil population. As such, the underlying contributions of individual neutrophil subsets to the overall response to a stimulus remains unresolved.

In conclusion, this work provided strong evidence that although similar morphologically, as seen by the common extrusion of cellular DNA, activation of neutrophils by PMA and ionomycin are two biochemical distinct processes that might exemplify distinct responses to the environment. Thus, PMA-activated neutrophils respond with the classical oxidative burst, and secreting proteins from all neutrophil granules, likely to kill the invading pathogen. On the other hand, ionomycin stimulation of neutrophils resembles pore-forming toxins released by microbials. In ionomycin-driven type of response, neutrophils quickly release their DNA extracellularly, and this event is preceded by the uncontrolled secretion of proteins from azurophilic and specific granules, and extensive protein citrullination. Importantly, proteins involved in NADPH oxidase complex formation, nuclear stability, and autoimmune pathologies were found citrullinated. This common mechanism of neutrophils response, independent of NADPH oxidase activation, may play a role in the development of autoimmune diseases.

CRediT authorship contribution statement

Lorenna Rocha Reis: Writing – review & editing, Writing – original draft, Methodology, Investigation, Formal analysis, Data curation. **Rafaela Oliveira Nascimento:** Writing – review & editing, Writing – original draft, Validation, Methodology, Investigation, Formal analysis, Data curation. **Mariana Pereira Massafera:** Writing – review & editing, Methodology, Formal analysis, Data curation. **Paolo Di Mascio:** Writing – review & editing, Investigation, Funding acquisition. **Graziella Eliza Ronsein:** Writing – review & editing, Writing – original draft, Supervision, Resources, Project administration, Methodology, Investigation, Funding acquisition, Formal analysis, Data curation, Conceptualization.

Funding

This study was financed by the São Paulo Research Foundation (FAPESP), Brasil, Process Numbers # 2012/12663-1, #2013/07937-8, #2016/00696-3, and #2023/00995-4. L.R.R and R.O.N. are recipients of FAPESP fellowship.

Declaration of competing interest

All authors declare there is no financial/personal interest or belief that could affect their objectivity. Authors do not have competing interests to declare.

Acknowledgments

The Redox Proteomics Core of the Mass Spectrometry Resource at Institute of Chemistry, University of São Paulo is acknowledged for access to MS instrumentation.

Appendix A. Supplementary data

Supplementary data to this article can be found online at https://doi.org/10.1016/j.redox.2025.103540.

Data availability

The mass spectrometry proteomics data have been deposited to the ProteomeXchange Consortium via the PRIDE partner repository with the dataset identifier PXD057968.

References

[1] C. Yin, B. Heit, Armed for destruction: formation, function and trafficking of neutrophil granules, Cell Tissue Res. 371 (2018) 455–471, https://doi.org/10.1007/s00441-017-2731-8.

[2] N. Borregaard, O.E. Sørensen, K. Theilgaard-Mönch, Neutrophil granules: a library of innate immunity proteins, Trends Immunol. 28 (2007) 340–345, https://doi.org/10.1016/j.it.2007.06.002.

[3] C.C. Winterbourn, A.J. Kettle, M.B. Hampton, Reactive oxygen species and neutrophil function, Annu. Rev. Biochem. 85 (2016) 765–792, https://doi.org/10.1146/annurev-biochem-060815-014442.

[4] N. Borregaard, J.B. Cowland, Granules of the human neutrophilic polymorphonuclear leukocyte, Blood 89 (1997) 3503–3521, https://doi.org/10.1182/blood.V89.10.3503.

[5] W.M. Nauseef, How human neutrophils kill and degrade microbes: an integrated view, Immunol. Rev. 219 (2007) 88–102, https://doi.org/10.1111/j.1600-065X.2007.00550.x.

[6] V. Brinkmann, U. Reichard, C. Goosmann, B. Fauler, Y. Uhlemann, D.S. Weiss, Y. Weinrauch, A. Zychlinsky, Neutrophil extracellular traps kill bacteria, Science 303 (2004) 1532–1535, https://doi.org/10.1126/science.1092385.

[7] B.E. Steinberg, S. Grinstein, Unconventional roles of the NADPH oxidase: signaling, ion homeostasis, and cell death, Sci. STKE 2007 (2007), https://doi.org/10.1126/stke.3792007pe11 pe11–pe11.

[8] I. Neeli, S.N. Khan, M. Radic, Histone deimination as a response to inflammatory stimuli in Neutrophils 1, J. Immunol. 180 (2008) 1895–1902, https://doi.org/10.4049/jimmunol.180.3.1895.

[9] Y. Wang, M. Li, S. Stadler, S. Correll, P. Li, D. Wang, R. Hayama, L. Leonelli, H. Han, S.A. Grigoryev, C.D. Allis, S.A. Coonrod, Histone hypercitrullination mediates chromatin decondensation and neutrophil extracellular trap formation, JCB (J. Cell Biol.) 184 (2009) 205–213, https://doi.org/10.1083/jcb.200806072.

[10] C.M. de Bont, W.J.H. Koopman, W.C. Boelens, G.J.M. Pruijn, Stimulus-dependent chromatin dynamics, citrullination, calcium signalling and ROS production during NET formation, Biochim. Biophys. Acta Mol. Cell Res. 1865 (2018) 1621–1629, https://doi.org/10.1016/j.bbamcr.2018.08.014.

[11] E.F. Kenny, A. Herzig, R. Krüger, A. Muth, S. Mondal, P.R. Thompson, V. Brinkmann, H. von Bernuth, A. Zychlinsky, Diverse stimuli engage different neutrophil extracellular trap pathways, Elife 6 (2017) e24437, https://doi.org/10.7554/eLife.24437.

[12] H. Parker, M. Dragunow, M.B. Hampton, A.J. Kettle, C.C. Winterbourn, Requirements for NADPH oxidase and myeloperoxidase in neutrophil extracellular trap formation differ depending on the stimulus, J. Leukoc. Biol. 92 (2012) 841–849, https://doi.org/10.1189/jlb.1211601.

[13] N.O. Christiansen, N. Borregaard, Translocation of protein kinase C to subcellular fractions of human neutrophils, Scand. J. Immunol. 29 (1989) 409–416, https://doi.org/10.1111/j.1365-3083.1989.tb01140.x.

[14] S.A. Belambri, L. Rolas, H. Raad, M. Hurtado-Nedelec, P.M.-C. Dang, J. El-Benna, NADPH oxidase activation in neutrophils: role of the phosphorylation of its subunits, Eur. J. Clin. Invest. 48 (2018) e12951, https://doi.org/10.1111/eci.12951.

[15] M. Faurschou, O.E. Sørensen, A.H. Johnsen, J. Askaa, N. Borregaard, Defensin-rich granules of human neutrophils: characterization of secretory properties, Biochim. Biophys. Acta Mol. Cell Res. 1591 (2002) 29–35, https://doi.org/10.1016/S0167-4889(02)00243-4.

[16] E. Neubert, D. Meyer, F. Rocca, G. Günay, A. Kwaczala-Tessmann, J. Grandke, S. Senger-Sander, C. Geisler, A. Egner, M.P. Schön, L. Erpenbeck, S. Kruss, Chromatin swelling drives neutrophil extracellular trap release, Nat. Commun. 9 (2018) 3767, https://doi.org/10.1038/s41467-018-06263-5.

[17] V. Papayannopoulos, K.D. Metzler, A. Hakkim, A. Zychlinsky, Neutrophil elastase and myeloperoxidase regulate the formation of neutrophil extracellular traps, JCB (J. Cell Biol.) 191 (2010) 677–691, https://doi.org/10.1083/jcb.201006052.

[18] K.D. Metzler, C. Goosmann, A. Lubojemska, A. Zychlinsky, V. Papayannopoulos, A myeloperoxidase-containing complex regulates neutrophil elastase release and actin dynamics during NETosis, Cell Rep. 8 (2014) 883–896, https://doi.org/10.1016/j.celrep.2014.06.044.

[19] R. Gennaro, T. Pozzan, D. Romeo, Monitoring of cytosolic free Ca2+ in C5a-stimulated neutrophils: loss of receptor-modulated Ca2+ stores and Ca2+ uptake in granule-free cytoplasts, Proc. Natl. Acad. Sci. U.S.A. 81 (1984) 1416–1420, https://doi.org/10.1073/pnas.81.5.1416.

[20] E. Tarcsa, L.N. Marekov, G. Mei, G. Melino, S.-C. Lee, P.M. Steinert, Protein unfolding by peptidylarginine deiminase: substrate specificity and structural relationships of the natural substrates trichohyalin and filaggrin, J. Biol. Chem. 271 (1996) 30709–30716, https://doi.org/10.1074/jbc.271.48.30709.

[21] H.R. Thiam, S.L. Wong, D.D. Wagner, C.M. Waterman, Cellular mechanisms of NETosis, Annu. Rev. Cell Dev. Biol. 36 (2020) 191–218, https://doi.org/10.1146/annurev-cellbio-020520-111016.

[22] M.F. Konig, F. Andrade, A critical reappraisal of neutrophil extracellular traps and NETosis mimics based on differential requirements for protein citrullination, Front. Immunol. 7 (2016), https://doi.org/10.3389/fimmu.2016.00461.

[23] S.S. Burgener, K. Schroder, Neutrophil extracellular traps in host defense, Cold Spring Harbor Perspect. Biol. 12 (2020) a037028, https://doi.org/10.1101/cshperspect.a037028.

[24] H. Zhong, R.-Y. Lu, Y. Wang, Neutrophil extracellular traps in fungal infections: a seesaw battle in hosts, Front. Immunol. 13 (2022), https://doi.org/10.3389/fimmu.2022.977493.

[25] B.M. Schultz, O.A. Acevedo, A.M. Kalergis, S.M. Bueno, Role of extracellular trap release during bacterial and viral infection, Front. Microbiol. 13 (2022), https://doi.org/10.3389/fmicb.2022.798853.

[26] V. Delgado-Rizo, M.A. Martínez-Guzmán, L. Iñiguez-Gutierrez, A. García-Orozco, A. Alvarado-Navarro, M. Fafutis-Morris, Neutrophil extracellular traps and its implications in inflammation: an overview, Front. Immunol. 8 (2017) 81. https://doi.org/10.3389/fimmu.2017.0008.

[27] G.S. Garcia-Romo, S. Caielli, B. Vega, J. Connolly, F. Allantaz, Z. Xu, M. Punaro, J. Baisch, C. Guiducci, R.L. Coffman, F.J. Barrat, J. Banchereau, V. Pascual, Netting neutrophils are major inducers of type I IFN production in pediatric systemic lupus erythematosus, Sci. Transl. Med. 3 (2011) 73ra20, https://doi.org/10.1126/scitranslmed.3001201.

[28] K. Kessenbrock, M. Krumbholz, U. Schönermarck, W. Back, W.L. Gross, Z. Werb, H.-J. Gröne, V. Brinkmann, D.E. Jenne, Netting neutrophils in autoimmune small-vessel vasculitis, Nat. Med. 15 (2009) 623–625, https://doi.org/10.1038/nm.1959.

[29] W.M. Nauseef, Isolation of human neutrophils from venous blood, in: M.T. Quinn, F.R. DeLeo, G.M. Bokoch (Eds.), Neutrophil Methods and Protocols, Humana Press, Totowa, NJ, 2007, pp. 15–20, https://doi.org/10.1007/978-1-59745-467-4_2.

[30] Y. Chen, W.G. Junger, Measurement of oxidative burst in neutrophils, Methods Mol. Biol. 844 (2012) 115, https://doi.org/10.1007/978-1-61779-527-5_8.

[31] L.R. Reis, D.R. Souza Junior, R. Tomasin, A. Bruni-Cardoso, P. Di Mascio, G. E. Ronsein, Citrullination of actin-ligand and nuclear structural proteins, cytoskeleton reorganization and protein redistribution across cellular fractions are early events in ionomycin-induced NETosis, Redox Biol. 64 (2023) 102784, https://doi.org/10.1016/j.redox.2023.102784.

[32] M. van der Linden, G.H.A. Westerlaken, M. van der Vlist, J. van Montfrans, L. Meyaard, Differential signalling and kinetics of neutrophil extracellular trap release revealed by quantitative live imaging, Sci. Rep. 7 (2017) 6529, https://doi.org/10.1038/s41598-017-06901-w.

[33] D. Pellerin, H. Gagnon, J. Dubé, F. Corbin, Amicon-adapted enhanced FASP: an in-solution digestion-based alternative sample preparation method to FASP. https://doi.org/10.12688/f1000research.6529.2, 2015.

[34] F.A. Gomes, D.R. Souza Junior, M.P. Massafera, G.E. Ronsein, Robust assessment of sample preparation protocols for proteomics of cells and tissues, Biochim. Biophys. Acta, Proteins Proteomics 1872 (2024) 141030, https://doi.org/10.1016/j.bbapap.2024.141030.

[35] J.R. Wiśniewski, Filter-aided sample preparation for proteome analysis, in: D. Becher (Ed.), Microbial Proteomics: Methods and Protocols, Springer, New York, NY, 2018, pp. 3–10, https://doi.org/10.1007/978-1-4939-8695-8_1.

[36] J. Cox, M. Mann, MaxQuant enables high peptide identification rates, individualized p.p.b.-range mass accuracies and proteome-wide protein quantification, Nat. Biotechnol. 26 (2008) 1367–1372, https://doi.org/10.1038/nbt.1511.

[37] J. Cox, N. Neuhauser, A. Michalski, R.A. Scheltema, J.V. Olsen, M. Mann, Andromeda: a peptide search engine integrated into the MaxQuant environment, J. Proteome Res. 10 (2011) 1794–1805, https://doi.org/10.1021/pr101065j.

[38] R. Chaerkady, Y. Zhou, J.A. Delmar, S.H.S. Weng, J. Wang, S. Awasthi, D. Sims, M. A. Bowen, W. Yu, L.H. Cazares, G.P. Sims, S. Hess, Characterization of citrullination sites in neutrophils and mast cells activated by ionomycin via integration of mass spectrometry and machine learning, J. Proteome Res. 20 (2021) 3150–3164, https://doi.org/10.1021/acs.jproteome.1c00028.

[39] J. Cox, M.Y. Hein, C.A. Luber, I. Paron, N. Nagaraj, M. Mann, Accurate proteome-wide label-free quantification by delayed normalization and maximal peptide ratio extraction, termed MaxLFQ, Mol. Cell. Proteomics 13 (2014) 2513–2526, https://doi.org/10.1074/mcp.M113.031591.

[40] S. Tyanova, T. Temu, P. Sinitcyn, A. Carlson, M.Y. Hein, T. Geiger, M. Mann, J. Cox, The Perseus computational platform for comprehensive analysis of (prote) omics data, Nat. Methods 13 (2016) 731–740, https://doi.org/10.1038/nmeth.3901.

[41] J. Goedhart, M.S. Luijsterburg, VolcaNoseR is a web app for creating, exploring, labeling and sharing volcano plots, Sci. Rep. 10 (2020) 20560, https://doi.org/10.1038/s41598-020-76603-3.

[42] Uku Raudvere, U. Raudvere, Liis Kolberg, L. Kolberg, I.V. Kuzmin, Ivan Kuzmin, I. V. Kuzmin, Ivan Kuzmin, T.V. Arak, T. Arak, Priit Adler, P. Adler, Hedi Peterson, H. Peterson, Jaak Vilo, J. Vilo, g:Profiler: a web server for functional enrichment analysis and conversions of gene lists (2019 update), Nucleic Acids Res. 47 (2019), https://doi.org/10.1093/nar/gkz369.

[43] B. Yates, B. Braschi, K.A. Gray, R.L. Seal, S. Tweedie, E.A. Bruford, Genenames.org: the HGNC and VGNC resources in 2017, Nucleic Acids Res. 45 (2017) D619–D625, https://doi.org/10.1093/nar/gkw1033.

[44] Y. Perez-Riverol, J. Bai, C. Bandla, D. García-Seisdedos, S. Hewapathirana, S. Kamatchinathan, D.J. Kundu, A. Prakash, A. Frericks-Zipper, M. Eisenacher, M. Walzer, S. Wang, A. Brazma, J.A. Vizcaíno, The PRIDE database resources in 2022: a hub for mass spectrometry-based proteomics evidences, Nucleic Acids Res. 50 (2021) D543, https://doi.org/10.1093/nar/gkab1038.

[45] J.M. Robinson, Reactive oxygen species in phagocytic leukocytes, Histochem. Cell Biol. 130 (2008) 281, https://doi.org/10.1007/s00418-008-0461-4.

[46] U. Jerke, S. Rolle, G. Dittmar, B. Bayat, S. Santoso, A. Sporbert, F. Luft, R. Kettritz, Complement receptor Mac-1 is an adaptor for NB1 (CD177)-mediated PR3-ANCA

neutrophil activation, J. Biol. Chem. 286 (2011) 7070–7081, https://doi.org/10.1074/jbc.M110.171256.
[47] S. Rørvig, O. Østergaard, N.H.H. Heegaard, N. Borregaard, Proteome profiling of human neutrophil granule subsets, secretory vesicles, and cell membrane: correlation with transcriptome profiling of neutrophil precursors, J. Leukoc. Biol. 94 (2013) 711–721, https://doi.org/10.1189/jlb.1212619.
[48] G. Alexandria, H.P. Valerio, M.P. Massafera, L.R. Reis, F.R. Coelho, P. Di Mascio, G. E. Ronsein, The miniaturized isolation of neutrophil granules (MING) method allowed a deep proteome mapping of human neutrophil granules, J. Leukoc. Biol. (2024), https://doi.org/10.1093/jleuko/qiae224 qiae224.
[49] P. Bouti, S.D.S. Webbers, S.C. Fagerholm, R. Alon, M. Moser, H.L. Matlung, T. W. Kuijpers, β2 Integrin signaling cascade in neutrophils: more than a single function, Front. Immunol. 11 (2020) 619925, https://doi.org/10.3389/fimmu.2020.619925.
[50] M. Lin, P. Jackson, A.M. Tester, E. Diaconu, C.M. Overall, J.E. Blalock, E. Pearlman, Matrix metalloproteinase-8 facilitates neutrophil migration through the corneal stromal matrix by collagen degradation and production of the chemotactic peptide Pro-Gly-Pro, Am. J. Pathol. 173 (2008) 144–153, https://doi.org/10.2353/ajpath.2008.080081.
[51] S. Rørvig, C. Honore, L.-I. Larsson, S. Ohlsson, C.C. Pedersen, L.C. Jacobsen, J. B. Cowland, P. Garred, N. Borregaard, Ficolin-1 is present in a highly mobilizable subset of human neutrophil granules and associates with the cell surface after stimulation with fMLP, J. Leukoc. Biol. 86 (2009) 1439–1449. https://doi.org/10.1189/jlb.1008606.
[52] B. Dewald, U. Bretz, M. Baggiolini, Release of gelatinase from a novel secretory compartment of human neutrophils. https://doi.org/10.1172/JCI110643, 1982.
[53] M. Leshner, S. Wang, C. Lewis, H. Zheng, X.A. Chen, L. Santy, Y. Wang, PAD4 mediated histone hypercitrullination induces heterochromatin decondensation and chromatin unfolding to form neutrophil extracellular trap-like structures, Front. Immunol. 3 (2012) 307. https://doi.org/10.3389/fimmu.2012.00307.
[54] I. Dupin, Y. Sakamoto, S. Etienne-Manneville, Cytoplasmic intermediate filaments mediate actin-driven positioning of the nucleus, J. Cell Sci. 124 (2011) 865–872, https://doi.org/10.1242/jcs.076356.
[55] A.E. Patteson, A. Vahabikashi, K. Pogoda, S.A. Adam, K. Mandal, M. Kittisopikul, S. Sivagurunathan, A. Goldman, R.D. Goldman, P.A. Janmey, Vimentin protects cells against nuclear rupture and DNA damage during migration, J. Cell Biol. 218 (2019) 4079–4092, https://doi.org/10.1083/jcb.201902046.
[56] A.L. Olins, A. Ernst, M. Zwerger, H. Herrmann, D.E. Olins, An in vitro model for Pelger-Huët anomaly, Nucleus 1 (2010) 506–512, https://doi.org/10.4161/nucl.1.6.13271.
[57] J. Camps, M.R. Erdos, T. Ried, The role of lamin B1 for the maintenance of nuclear structure and function, Nucleus 6 (2015) 8–14, https://doi.org/10.1080/19491034.2014.1003510.
[58] A. Panday, M.K. Sahoo, D. Osorio, S. Batra, NADPH oxidases: an overview from structure to innate immunity-associated pathologies, Cell. Mol. Immunol. 12 (2015) 5–23, https://doi.org/10.1038/cmi.2014.89.
[59] Y. Zhou, L.-L. An, R. Chaerkady, N. Mittereder, L. Clarke, T.S. Cohen, B. Chen, S. Hess, G.P. Sims, T. Mustelin, Evidence for a direct link between PAD4-mediated citrullination and the oxidative burst in human neutrophils, Sci. Rep. 8 (2018) 15228, https://doi.org/10.1038/s41598-018-33385-z.
[60] E.E. Witalison, P.R. Thompson, L.J. Hofseth, Protein arginine deiminases and associated citrullination: physiological functions and diseases associated with dysregulation, Curr. Drug Targets 16 (2015) 700–710.
[61] R. Tilvawala, S.H. Nguyen, A.J. Maurais, V.V. Nemmara, M. Nagar, A.J. Salinger, S. Nagpal, E. Weerapana, P.R. Thompson, The rheumatoid arthritis-associated citrullinome, Cell Chem. Biol. 25 (2018) 691–704.e6, https://doi.org/10.1016/j.chembiol.2018.03.002.
[62] E. Darrah, F. Andrade, Rheumatoid arthritis and citrullination, Curr. Opin. Rheumatol. 30 (2018) 72, https://doi.org/10.1097/BOR.0000000000000452.
[63] A.E.V. Tutturen, B. Fleckenstein, G.A. de Souza, Assessing the citrullinome in rheumatoid arthritis synovial fluid with and without enrichment of citrullinated peptides, J. Proteome Res. 13 (2014) 2867–2873, https://doi.org/10.1021/pr500030x.
[64] V. Romero, J. Fert-Bober, P.A. Nigrovic, E. Darrah, U.J. Haque, D.M. Lee, J. van Eyk, A. Rosen, F. Andrade, Immune-Mediated pore-forming pathways induce cellular hypercitrullination and generate citrullinated autoantigens in rheumatoid arthritis, Sci. Transl. Med. 5 (2013), https://doi.org/10.1126/scitranslmed.3006869, 209ra150-209ra150.
[65] R.D. Estensen, J.G. White, B. Holmes, Specific degranulation of human polymorphonuclear leukocytes, Nature 248 (1974) 347–348, https://doi.org/10.1038/248347a0.
[66] J.E. Repine, J.G. White, C.C. Clawson, B.M. Holmes, The influence of phorbol myristate acetate on oxygen consumption by polymorphonuclear leukocytes, J. Lab. Clin. Med. 83 (1974) 911–920.
[67] D.G. Wright, D.A. Bralove, J.I. Gallin, The differential mobilization of human neutrophil granules. Effects of phorbol myristate acetate and ionophore A23187, Am. J. Pathol. 87 (1977) 237.
[68] P. Li, M. Li, M.R. Lindberg, M.J. Kennett, N. Xiong, Y. Wang, PAD4 is essential for antibacterial innate immunity mediated by neutrophil extracellular traps, J. Exp. Med. 207 (2010) 1853–1862, https://doi.org/10.1084/jem.20100239.
[69] T.A. Fuchs, U. Abed, C. Goosmann, R. Hurwitz, I. Schulze, V. Wahn, Y. Weinrauch, V. Brinkmann, A. Zychlinsky, Novel cell death program leads to neutrophil extracellular traps, J. Cell Biol. 176 (2007) 231–241, https://doi.org/10.1083/jcb.200606027.
[70] D.N. Douda, M.A. Khan, H. Grasemann, N. Palaniyar, SK3 channel and mitochondrial ROS mediate NADPH oxidase-independent NETosis induced by calcium influx, Proc. Natl. Acad. Sci. USA 112 (2015) 2817–2822, https://doi.org/10.1073/pnas.1414055112.
[71] A.S. Byrd, X.M. O'Brien, C.M. Johnson, L.M. Lavigne, J.S. Reichner, An extracellular matrix-based mechanism of rapid neutrophil extracellular trap formation in response to C. albicans, J. Immunol. 190 (2013) 4136–4148, https://doi.org/10.4049/jimmunol.1202671.
[72] K. Chen, H. Nishi, R. Travers, N. Tsuboi, K. Martinod, D.D. Wagner, R. Stan, K. Croce, T.N. Mayadas, Endocytosis of soluble immune complexes leads to their clearance by FcγRIIIB but induces neutrophil extracellular traps via FcγRIIA in vivo, Blood 120 (2012) 4421–4431, https://doi.org/10.1182/blood-2011-12-401133.
[73] H.R. Thiam, S.L. Wong, R. Qiu, M. Kittisopikul, A. Vahabikashi, A.E. Goldman, R. D. Goldman, D.D. Wagner, C.M. Waterman, NETosis proceeds by cytoskeleton and endomembrane disassembly and PAD4-mediated chromatin decondensation and nuclear envelope rupture, Proc. Natl. Acad. Sci. USA 117 (2020) 7326–7337, https://doi.org/10.1073/pnas.1909546117.
[74] H.D. Lewis, J. Liddle, J.E. Coote, S.J. Atkinson, M.D. Barker, B.D. Bax, K.L. Bicker, R.P. Bingham, M. Campbell, Y.H. Chen, C. Chung, P.D. Craggs, R.P. Davis, D. Eberhard, G. Joberty, K.E. Lind, K. Locke, C. Maller, K. Martinod, C. Patten, O. Polyakova, C.E. Rise, M. Rüdiger, R.J. Sheppard, D.J. Slade, P. Thomas, J. Thorpe, G. Yao, G. Drewes, D.D. Wagner, P.R. Thompson, R.K. Prinjha, D. M. Wilson, Inhibition of PAD4 activity is sufficient to disrupt mouse and human NET formation, Nat. Chem. Biol. 11 (2015) 189–191, https://doi.org/10.1038/nchembio.1735.
[75] J.C. Jennette, H. Xiao, R.J. Falk, Pathogenesis of vascular inflammation by anti-neutrophil cytoplasmic antibodies, J. Am. Soc. Nephrol. JASN 17 (2006) 1235–1242. https://doi.org/10.1681/ASN.2005101048.
[76] J. Liu, J. Gao, Z. Wu, L. Mi, N. Li, Y. Wang, X. Peng, K. Xu, F. Wu, L. Zhang, Anti-citrullinated protein antibody generation, pathogenesis, clinical application, and prospects, Front. Med. 8 (2022), https://doi.org/10.3389/fmed.2021.802934.
[77] M.F. Konig, L. Abusleme, J. Reinholdt, R.J. Palmer, R.P. Teles, K. Sampson, A. Rosen, P.A. Nigrovic, J. Sokolove, J.T. Giles, N.M. Moutsopoulos, F. Andrade, Aggregatibacter actinomycetemcomitans–induced hypercitrullination links periodontal infection to autoimmunity in rheumatoid arthritis, Sci. Transl. Med. 8 (2016), https://doi.org/10.1126/scitranslmed.aaj1921, 369ra176-369ra176.
[78] N. Malachowa, S.D. Kobayashi, B. Freedman, D.W. Dorward, F.R. DeLeo, Staphylococcus aureus leukotoxin GH promotes formation of neutrophil extracellular traps, J. Immunol. 191 (2013) 6022–6029, https://doi.org/10.4049/jimmunol.1301821.
[79] R.H.P. Law, N. Lukoyanova, I. Voskoboinik, T.T. Caradoc-Davies, K. Baran, M. A. Dunstone, M.E. D'Angelo, E.V. Orlova, F. Coulibaly, S. Verschoor, K.A. Browne, A. Ciccone, M.J. Kuiper, P.I. Bird, J.A. Trapani, H.R. Saibil, J.C. Whisstock, The structural basis for membrane binding and pore formation by lymphocyte perforin, Nature 468 (2010) 447–451, https://doi.org/10.1038/nature09518.
[80] I. Osińska, K. Popko, U. Demkow, Perforin: an important player in immune response, Cent. Eur. J. Immunol. 39 (2014) 109–115, https://doi.org/10.5114/ceji.2014.42135.
[81] C. Silvestre-Roig, A. Hidalgo, O. Soehnlein, Neutrophil heterogeneity: implications for homeostasis and pathogenesis, Blood 127 (2016) 2173–2181, https://doi.org/10.1182/blood-2016-01-688887.
[82] M.F. Denny, S. Yalavarthi, W. Zhao, S.G. Thacker, M. Anderson, A.R. Sandy, W. J. McCune, M.J. Kaplan, A distinct subset of proinflammatory neutrophils isolated from patients with systemic lupus erythematosus induces vascular damage and synthesizes type I IFNs, J. Immunol. 184 (2010) 3284–3297, https://doi.org/10.4049/jimmunol.0902199.
[83] M. Hassani, P. Hellebrekers, N. Chen, C. van Aalst, S. Bongers, F. Hietbrink, L. Koenderman, N. Vrisekoop, On the origin of low-density neutrophils, J. Leukoc. Biol. 107 (2020) 809–818, https://doi.org/10.1002/JLB.5HR0120-459R.
[84] E. Villanueva, S. Yalavarthi, C.C. Berthier, J.B. Hodgin, R. Khandpur, A.M. Lin, C. J. Rubin, W. Zhao, S.H. Olsen, M. Klinker, D. Shealy, M.F. Denny, J. Plumas, L. Chaperot, M. Kretzler, A.T. Bruce, M.J. Kaplan, Netting neutrophils induce endothelial damage, infiltrate tissues and expose immunostimulatory molecules in systemic lupus erythematosus, J. Immunol. 187 (2011) 538–552, https://doi.org/10.4049/jimmunol.1100450.